Supplemental Material for: *Pressure Tensor Elements Breaking the Frozen-In Law During Reconnection in Earth's Magnetotail.*

J. Egedal[1], J. Ng[2], A. Le[3], W. Daughton[3], B. Wetherton[1], J. Dorelli[4], D. Gershman[4], and A. Rager[4]
[1] *Department of Physics, University of Wisconsin-Madison, Madison, Wisconsin 53706, USA*
[2] *Center for Heliophysics, Princeton Plasma Physics Laboratory, Princeton NJ 08543, USA*
[3] *Los Alamos National Laboratory, Los Alamos, New Mexico 87545, USA and*
[4] *Heliophysics Science Division, NASA Goddard Space Flight Center, Greenbelt, Maryland 20771, USA*
(Dated: August 22, 2019)

In this supplement to the Letter referenced in the title, we detail the methods by which we determined the upstream plasma parameters required for numerical simulation of the July 11, 2017 magnetotail reconnection event. For quantitative comparison between the simulation and MMS data, we derive a normalization scheme for translating the natural simulation units into the units of MMS. Finally, we describe the optimization method by which we determined the best trajectory through the simulation for matching the time-series data recorded by MMS.

I. GENERAL METHODOLOGY

The aim of the Letter is in part to determine to what extent the details of the MMS observations of magnetotail reconnection during the event of July 11, 2017 can be accounted for by 2D kinetic simulation. In our numerical reconstruction of the event, the path of MMS through the 2D simulation is largely determined by the time series of the magnetic field recorded by MMS. The magnetic field measurements include fluctuations with an amplitude of about $0.3\,\mathrm{nT}$ at frequencies up to $2\,\mathrm{Hz}$. Thus, the characteristic fluctuation frequency is slow compared to the typical transit frequency of electrons traversing the full length of the electron diffusion region (EDR), $f_t = v_{the}/L_{\mathrm{EDR}} \simeq (2\cdot 10^7 \mathrm{m\,s^{-1}})/10^6\mathrm{m} \simeq 20\,\mathrm{Hz}$. This difference in time scales motivates our assumption that the magnetic perturbations are caused by external Alfvénic activity driving variations in the N-coordinate of reconnection layer relative to the MMS spacecraft.

During the $\sim 10\,\mathrm{s}$ time interval considered, as the x-line retreats $\sim 2\cdot 10^6\,\mathrm{m}$ in the tail-ward direction, from the magnetic perturbations we find that the MMS path fluctuates by about $\sim 6\cdot 10^4\,\mathrm{m}$ in the N-direction normal to the reconnection current layer. While the Alfvénic activity responsible for these fluctuations may well be 3D in nature, our analysis implies that the detailed features recorded in and around the EDR are well accounted for by evaluating 2D simulation quantities along a path dictated by the recorded magnetic field time-series (including the $\lesssim 2\,\mathrm{Hz}$ perturbations). As such, the data appear consistent with a "ridged" 2D reconnection geometry pushed slightly back and forth in the N-direction by Alfvénic activity external to the EDR.

In general, we find that the task of numerically reconstructing an *in situ* spacecraft event can be divided into seven separate steps.

1. Determine upstream initial plasma parameters needed for implementing the initial plasma conditions and carry out the fully kinetic reconnection simulation.
2. For quantitative comparisons, translate the kinetic simulation units into the units used by MMS.
3. Pick a trial set of LMN basis vectors, and rotate the MMS data from GSE coordinates to determine the times series for the LMN components of all relevant vector and tensor quantities.
4. Infer the trajectory through the simulation that matches the time-series of B_L and B_N recorded by MMS (we used B_L and B_N of MMS1). Note that this step is rigorously defined given the simulation profiles of B_L and B_N have been translated into the units used by MMS (nT).
5. Reconstruct all relevant event data by evaluating simulation quantities along the inferred trajectory through the simulation.
6. Repeat steps 3 to 5 to search and isolate the LMN basis vectors that provide the best visual agreement between the MMS observations and simulation quantities. These quantities include B_M and the vector components of $\mathbf{u}_e$ and $\mathbf{E}$. To provide unbiased reconstruction of the electron pressure tensor, the electron pressure elements were not included for the optimization described under this step.
7. Based on the overall agreement between the optimized reconstructed profiles and the MMS observations, decide if the initial numerical plasma parameters of step 1 were representative for the event. If not, repeat steps 1 to 6.

The details of how a range of these steps are completed are sensitive to the specific nature of the data series recorded by the spacecraft. In particular, for the present event many different strategies were attempted when completing step 6. Our summary below includes a description of the approach taken for each step, including our final strategy for step 6 that helped simplify the search for an optimized set of LMN basis vectors.

II. UPSTREAM PLASMA PARAMETERS

In the Earth's magnetotail EDRs typically retreat in the tailward direction. Thus, in fortuitous *in situ* EDR encounters the spacecraft will generally sample the two exhaust regions (separated by the EDR) without making direct contact with the upstream plasma feeding the two inflow regions. Without such direct measurements, the upstream plasma conditions must be inferred by other methods. In particular, numerical simulations require the specification of the normalized upstream pressures for both the electrons and the ions, $\beta_{e\infty}$ and $\beta_{i\infty}$.

For the present event MMS sampled a region of strong electron pressure anisotropy, $T_{e\|} \simeq 4T_{e\perp}$, a few d_e upstream of the EDR. Over the past decade a detailed theory has been developed which predicts this anisotropy level as a function of $\beta_{e\infty}$. Using the theoretical scaling laws of [Le *et al.*, Phys. Plasma, **23**, 2016] we obtained the estimate that $\beta_{e\infty} \simeq 0.045$. Furthermore, in the work by Le *et al.* theoretical scaling laws are also available for the relative electron heating observed from the inflow region to the exhaust region just downstream of the EDR (where for this event $T_e \simeq 820\,\mathrm{eV}$). For $\beta_{e\infty} \simeq 0.045$ the relative heating factor is $\simeq 1.7$ corresponding to an upstream electron temperature of $T_{e\infty} \simeq 820\,\mathrm{eV}/1.7 \simeq 480\,\mathrm{eV}$. Assuming that the ion temperature near the EDR, $T_i \simeq 5\,\mathrm{keV}$ is representative for the upstream conditions, we estimate the normalized upstream ion pressure to be $\beta_{i\infty} \simeq 10\,\beta_{e\infty} \simeq 0.45$.

Besides these estimates for $\beta_{e\infty}$ and $\beta_{i\infty}$, the kinetic simulations also required specification of the upstream guide magnetic field $B_{M\infty}$ relative to $B_{L\infty}$. Based on the analysis in [Torbert *et al.*, Science, 2018] we first carried out a simulation with $B_{M\infty} = 0$. As will discussed further below, we carried out two additional simulations with $B_{M\infty}/B_{L\infty} = 0.02$ and 0.006 to optimize the agreement between MMS and the numerical reconstruction. The simulation detailed in the Letter applied the latter value ($B_{M\infty}/B_{L\infty} = 0.006$), representing our best estimate for the guide field. While this value may appear negligible, it turns out to have a strong impact on the numerical profiles of E_N, providing further evidence for the presence of this small but finite level of the guide field.

III. CONVERSION OF SIMULATION UNITS

For numerical tractability fully kinetic simulations of reconnection nearly always apply reduced values of m_i/m_e and ω_{pe}/ω_{ce}, and it follows that it is generally not possible to define a true mapping from the "natural" simulation units to the units applied by MMS. However, in the present study we applied the natural proton to electron mass ratio $m_i/m_e = 1836$, and only ω_{pe}/ω_{ce} was assigned an unphysical value, $\omega_{pe}/\omega_{ce} = 2$. Correspondingly, because β_e is critical to the reconnection physics, the kinetic simulations employ an unphysically larger value of $v_{the}/c = \lambda_D/d_e \sim 0.1$, so that $\beta_e = ((\omega_{pe}/\omega_{ce})(v_{the}/c))^2$ matches the observations. Because $c = 1/\sqrt{\mu_0\epsilon_0}$, the reduced value of ω_{pe}/ω_{ce} is then equivalent to an enhanced numerical value of the vacuum permittivity, ϵ_0.

Based on the principle of plasma quasi-neutrality, electric fields within an electron-proton plasma develop to maintain nearly identical values of the electron and ion number densities, $n_e \simeq n_i$. Plasma dynamics at length scales larger than the Debye scale, $\lambda_{De} = v_{the}\,\omega_{pe}$, can then be shown to be independent of the actual value of ϵ_0. In fact, this principle is extensively used in fluid models where Poisson's equation is eliminated and replaced by the constraint $n_e = n_i$. This motivated our normalization scheme below which is deliberately insensitive to the numerical value of ϵ_0.

We find that there are two free parameters to be determined to set the transformation of the simulation units. We choose these parameters to be α_n and α_T, introduced to match the density and temperature profiles in Figs. 1(a,b,k,l) of the Letter,

$$\alpha_n \equiv \frac{n_{\mathrm{MMS}}}{n_{\mathrm{VPIC}}} = \frac{0.047\,\mathrm{cm}^{-3}}{0.75}\,, \quad \alpha_T \equiv \frac{T_{\mathrm{MMS}}}{T_{\mathrm{VPIC}}} = \frac{820\,\mathrm{eV}}{0.021} \quad .$$

With α_n and α_T determined, the conversions of all other VPIC quantities to "MMS units" are now fixed. For example, using the electron skin depth $d_e = \sqrt{m_e/(\mu_0 n_e e^2)}$ as the fundamental length scale, equivalent normalization of plasma pressures $2\mu_0 nT/B^2$, work by electric fields eEd_e/T_e, and kinetic energy $m_e v^2/(2T_e)$ require the conversion ratios

$$\frac{B_{\mathrm{MMS}}}{B_{\mathrm{VPIC}}} = \sqrt{\mu_0\alpha_n\alpha_T}\,, \quad \frac{v_{\mathrm{MMS}}}{v_{\mathrm{VPIC}}} = \sqrt{\frac{\alpha_T}{m_e}}\,,$$

$$\frac{E_{\mathrm{MMS}}}{E_{\mathrm{VPIC}}} = \alpha_T\sqrt{\frac{\mu_0\alpha_n}{m_e}}\,, \quad \frac{P_{\mathrm{MMS}}}{P_{\mathrm{VPIC}}} = \alpha_n\alpha_T\,.$$

With these ratios determined we established a unique mapping of the simulation units to the units applied by MMS. This mapping then facilitated the quantitative comparison between the MMS observations and the simulations, the success of which confirms the principle of quasi-neutrality and also indicates that Debye scale physics do not play a key role for setting the structure of the observed EDR.

IV. DETERMINING THE LMN BASIS VECTORS OF THE EVENT

For reconnection events where the two inflow regions are sampled by the spacecraft, standard minimum variance analysis methods are available for estimating the LMN basis vectors of the event. For the present event, however, where the directions and strengths of the upstream magnetic fields were not measured, we rely on the result of the kinetic simulations and an iterative approach (outlined above in step 6 of Section I) to estimate the direction of the LMN basis unit vectors (expressed in GSE coordinates).

We applied a range of strategies for this optimization. Ultimately, the task was considerably reduced by using the strong variations in $\mathbf{E}$ to set the $\mathbf{N}$-direction. As is evident from the simulation profiles displayed in the Letter, only E_N depends strongly on the N-coordinate, and the abrupt changes in the measured $\mathbf{E}$ at $t \simeq 3\,\mathrm{s}$ must therefore lie in the N-direction. This observation provided our estimate for the N-direction, differing by about $10°$ from the N-direction of [Torbert *et al.*, Science, 2018].

With the N-direction fixed the MMS time profile of B_N is known. Furthermore, changes in the electron distribution functions identified the beginning and the end of the EDR. The three vertical dashed lines in the panels of Fig. 1 of the Letter mark the beginning, $B_N = 0$, and the end of the EDR, respectively. The time asymmetry of these lines could be caused by the X-line being located tail-ward within the EDR. Here, however, we match the asymmetry (and recorded B_N) by assuming that the relative N-velocity of MMS slowed by a factor of about 3 during the second half of the EDR encounter. Timing analysis of the $B_N = 0$ crossings of MMS1 and MMS4 indicates a tail-ward retreat of the X-line at $v_{xL} = -230\,\mathrm{km\,s^{-1}}$, corresponding to a half length of the EDR of about $15d_e$. Given the knowledge of the N-direction we were thus able to estimate the L coordinate of the MMS spacecraft as a function of time, $L_{\mathrm{MMS}}(t)$.

The described determination of the N-direction, of course, also helps determine $\mathbf{L}$ and $\mathbf{M}$, as these lie in the plane perpendicular to $\mathbf{N}$, and the possible choices for $\mathbf{L}$ and $\mathbf{M}$ are then parameterized in terms of a single angle. For each choice of this angle, $B_L(t)$ is fixed, and a path through the simulation domain is uniquely determined by $B_L(t)$ and $L_{\mathrm{MMS}}(t)$. Optimizing the reconstructed profiles to match those recorded by MMS yielded the unit vectors applied in the Letter and listed here in GSE coordinates: $[\mathbf{L};\mathbf{M};\mathbf{N}] = [0.94, -0.35, -0.03; 0.32, 0.90, -0.33; 0.15, 0.30, 0.94]$. The uncertainty for each direction is estimated to be about five degrees.

The basis vectors estimated in [Torbert *et al.*, Science, 2018] were in part determined by minimum variance analysis of the electron flow within the EDR. We find, however, that MMS mostly sampled the Earthward part of the electron outflow jets, likely impacting the accuracy of the method. In turn, this provides an explanation for the relatively large discrepancy ($\simeq 33°$) between our L and M directions compared to those of Torbert *et al.*.

V. INFERRING THE UPSTREAM GUIDE MAGNETIC FIELD

The upstream guide magnetic field $B_{M\infty} = 0.006$ was determined by an iteration of simulations as outlined in Step 7 of Section I. This was particularly important for the features near $t \simeq 3\,\mathrm{s}$ related to the strength of B_M in comparison to B_L. In this region within the EDR where $N \simeq 0$ and $L > 0$ the simulation with $B_{M\infty} = 0$ suggested that $B_M \simeq B_L/2$. However, from MMS data in Figs. 1(d,e) of the Letter we observe that $B_M \simeq B_L/2 + 0.5nT$. To match this offset we carried out two additional simulations iterating the upstream guide magnetic field. The value of $B_{M\infty}/B_{L\infty} = 0.02$ represented a clear overcorrection to the first run at $B_{M\infty} = 0$, but allowed us to interpolate to $B_{M\infty}/B_{L\infty} = 0.006$ of the final VPIC run presented in the Letter.

The small but finite guide magnetic field has important impact on the profile of E_N. In Fig. 1(a) below we present E_N for $B_{M\infty} = 0$, while in Fig. 1(b) the profile is for $B_{M\infty}/B_{L\infty} = 0.006$. For $B_{M\infty} = 0$, the profile of E_N reverses sign three times as the reconnection layer is crossed. This triple sign reversal is not compatible with the recorded times series of E_N by MMS3 presented in Fig. 1(i) of the Letter. In contrast the profile of E_N for $B_{M\infty}/B_{L\infty} = 0.006$ only has a single sign reversal significantly improving the match between the measured and reconstructed profiles recorded by MMS3 of E_N displayed in Figs. 1(i,t) in the Letter.

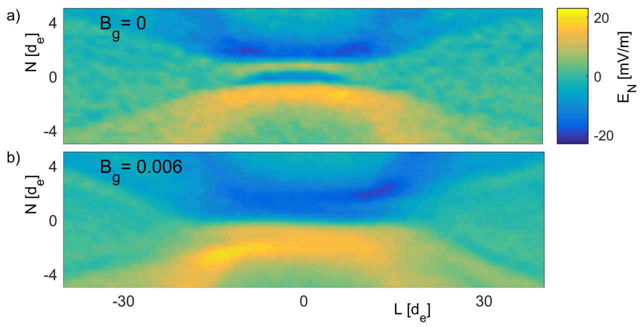

FIG. 1: E_N electric field profiles observed in a) for $B_g = B_{M\infty}/B_{L\infty} = 0$ and in b) for $B_g = B_{M\infty}/B_{L\infty} = 0.006$. The profile in b) yields better agreement with the MMS data.